

resulted in an extent of bioavailability of at least that of the standard. The *in vitro* test revealed acceptable tablet properties with respect to weight uniformity, friability, and *in vitro* drug release. Considering the simple methodology employed in the manufacturing of direct compression tablets, this technique and the direct compression mass tested have a high potential for commercial use of a quality product.

REFERENCES

- (1) Publication No. 76-3009, Department of Health, Education, and Welfare, Public Health Service, Rockville, Md., Jan. 1976.
- (2) K. J. Randeri, *Diss. Abstr.*, **25**, 7212 (1965).
- (3) P. D. Sheth and O. Nuessle, Ph.D. dissertation, University of Missouri, Kansas City, Mo., 1971.
- (4) D. Schickling, M.S. thesis, University of Cincinnati, Cincinnati, Ohio, 1972.
- (5) M. R. Scheffler and W. A. Ritschel, *Pharm. Ind.*, **37**, 511 (1975).

- (6) W. Erni and W. A. Ritschel, *ibid.*, **39**, 284 (1977).
- (7) *Ibid.*, in press.
- (8) G. R. VanPetten, G. C. Becking, R. J. Withey, and H. F. Lettan, *J. Clin. Pharmacol.*, **11**, 27 (1971).
- (9) W. A. Ritschel, G. Ritschel, C. R. Buncher, and J. Rotmensch, *Drug Intel. Clin. Pharm.*, **10**, 401 (1976).
- (10) K. A. Khan and C. T. Rhodes, *Pharm. Acta Helv.*, **51**, 23 (1976).
- (11) E. Reimerdes and J. H. Thumin, *Arzneim.-Forsch.*, **20**, 1176 (1970).
- (12) A. C. Bratton and E. K. Marshall, Jr., *J. Biol. Chem.*, **128**, 537 (1939).

ACKNOWLEDGMENTS AND ADDRESSES

Received July 30, 1976, from the College of Pharmacy, University of Cincinnati Medical Center, Cincinnati, OH 45267.

Accepted for publication January 3, 1977.

* To whom inquiries should be directed.

Mathematical Model for Cyclocytidine Pharmacokinetics

K. J. HIMMELSTEIN *^x and J. F. GROSS †

Abstract □ The pharmacokinetics of the drug cyclocytidine in humans were modeled by using a physiological and anatomical approach. Each pertinent tissue is represented by a single compartment, and these compartments are linked together by the circulatory system. Each compartment is then represented by an ordinary differential equation that represents the rate of change in drug concentration as a function of convecting transport, metabolism, and urinary clearance. The models for cyclocytidine and cytarabine are linked together by a hydrolysis term in each equation set. The resulting equation sets are then solved numerically to predict the concentration of both drug species *in situ*. The models use physiological blood flows, tissue volumes, and clearance parameters. The results of the model show that cyclocytidine can act as a reservoir for cytarabine *in vivo* over the time studied. This effect is confined to relatively long times and relatively low plasma concentrations.

Keyphrases □ Cyclocytidine—pharmacokinetics in humans, mathematical model □ Pharmacokinetics—cyclocytidine in humans, mathematical model □ Models, mathematical—cyclocytidine pharmacokinetics in humans

Cytarabine (I) (NSC-63878), an effective antileukemic agent (1–3), has a very short half-life because of its rapid deamination to a biologically inactive compound. *O*²,*2'*-Cyclocytidine (II) (NSC-145688), which is structurally similar to I, was more effective than I in several animal tumor systems (4, 5). The efficacy of II may be due to its hydrolysis to I (6). If so, its effects may be strongly related to the pharmacokinetics of both I and II *in vivo*.

The enhanced cytotoxic effect of II could possibly be due to its slower urinary clearance compared to the elimination of I by deamination and kidney clearance. Thus, II could act as a reservoir for the production of I *in vivo*. This paper presents a mathematical model to study the distribution and hydrolysis of II to I *in vivo*. This model demonstrates that the pharmacokinetic characteristics of II are important to its effective usage.

PHARMACOKINETIC MODEL

The model, an extension of the work by Dedrick *et al.* (7, 8), is based on the principle that anatomical and physiological parameters should be included to reflect biochemical interactions of the drug. The rationale for modeling on this basis as opposed to classical compartmental analysis was developed previously (9–15).

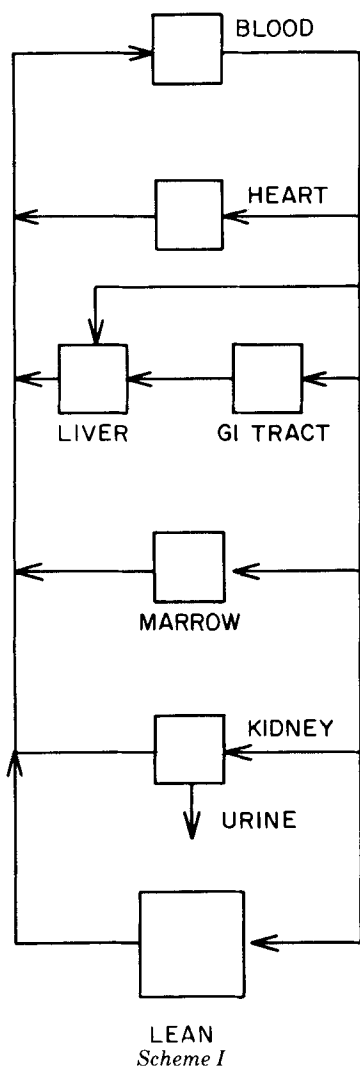
By using compartments to represent real organs, the actual blood flows and physiological volumes as well as terms to include metabolism, urinary clearance, and binding can be included. Thus, when the model is complete, it can provide predictive capability derived from a quantitative physiological and pharmacological basis. Since a model for the pharmacokinetics of I was described in detail (7, 8, 16), only key assumptions that deal directly with changes for the inclusion of II are discussed.

Scheme I represents the flow diagram of the various compartments used in the model. Each compartment represents a real organ, with the anatomical volume experimentally measured independently. The organs are contained in a network representing the systemic blood circulation. The blood flows are also measured independently for each compartment. A drug mass balance represents the rate of change of the mass of drug in the compartment as a function of the convective inflow and outflow rates, the metabolism rate, the elimination rate by urinary or other clearance, and the rate of drug introduction from external sources.

Dedrick *et al.* (7, 8) used the following assumptions to write differential equations describing the pharmacokinetics of I. Each organ is a volume of distribution for the drug, and deamination can be represented by a Michaelis–Menten expression. Urinary clearance is directly proportional to the concentration in the blood. For II, a similar compartmental network is considered. Since the chemical structures of II and I are closely related, it is assumed that they will act similarly, with no gross differences in distribution and urinary clearance from the body.

Compound II is not deaminated *in vivo* (17), and hydrolysis of II to I is assumed to take place in all tissues. Thus, a production term for I is included in each balance that is first order in II concentration (16). The balance equation on the blood compartment for I is:

$$V_B \frac{dC_B}{dt} = Q_H C_H + Q_{Li} C_{Li} + Q_M C_M + Q_K C_K + Q_{Le} C_{Le} - Q_B C_B - \frac{V_{max,B} C_B}{K_{m,B} + C_B} V_B + Mg(t) + K_h X_B \phi V_B \quad (\text{Eq. 1})$$



Scheme I

where V represents the compartment size in milliliters, C represents the concentration of I in milligrams per milliliter, Q is the blood flow rate in milliliters per minute, K_h is the I urinary clearance in milliliters per minute, V_{max} is the deamination activity at saturation in micrograms per minute, and K_m represents the Michaelis constant in micrograms per milliliter. The subscripts represent each compartment: H , heart; L , liver; M , marrow; K , kidney; Le , lean; and B , blood. The term X represents the concentration of II in various compartments, M is the total dose of drug injected, $g(t)$ is the injection function, K_h is the hydrolysis rate constant, K_c is the kidney clearance of II, ϕ represents the ratio of the molecular weights of I to II, and t represents time. A sample equation for I for one compartment (the kidney) is given by:

$$V_K \frac{dC_K}{dt} = Q_K C_B - Q_K C_K - K_K C_B - \frac{V_{max,K} C_K}{K_{m,K} + C_K} V_K + K_h V_K \phi X_K \quad (\text{Eq. 2})$$

Equation 3 represents the mass balance of II in the blood compartment:

$$V_B \frac{dX_B}{dt} = Q_H X_H + Q_{Li} X_{Li} + Q_M X_M + Q_K X_K + Q_{Le} X_{Le} + Mg(t) - K_h X_B V_B \quad (\text{Eq. 3})$$

Equation 4 represents a typical compartment (the kidney) for II:

$$V_K \frac{dX_K}{dt} = Q_K X_B - Q_K X_K - K_C X_B - K_h X_K V_K \quad (\text{Eq. 4})$$

A similar balance in each compartment for both II and I is made, resulting in a set of ordinary nonlinear differential equations to be solved simultaneously and numerically on a digital computer. When the equations are solved, the results are the time-dependent concentrations for

Table I—Model Parameters for Cycloctidine Pharmacokinetic Model

Parameter	Value in Humans	Reference
Body weight, g	70,000	7
Volume, V , ml		
Blood	2,670	7
Liver	1,700	7
Gut	3,180	7
Heart	450	7
Kidneys	1,060	7
Lean	27,000	7
Marrow	2,000	7
Blood Flow, Q , ml/min		
Cardiac output (for model)	4,040	7
Liver	1,450	7
Gut	1,100	7
Heart	240	7
Kidneys	1,240	7
Lean	930	7
Marrow	180	7
Michaelis constant, K_m , $\mu\text{g/ml}$		
Heart	31	8
Liver	27	20
Kidneys	32	8
Deaminase activity, V_{max} , $\mu\text{g/g min}$		
Liver	119	19
Heart	6	20
Kidneys	20	20
Clearance, K_c , K_k , ml/min		
I	90	8
II	70	14
Hydrolysis rate, min^{-1} ^a	0.01(0.005) ^a	

^a *In vitro* calculation from Ref. 16.

each drug in each tissue compartment plus the blood compartment and the total urinary excretion, which is given for I by:

$$U_I = \int_0^t K_k C_B dt' \quad (\text{Eq. 5a})$$

and for II by:

$$U_{II} = \int_0^t K_c X_B dt' \quad (\text{Eq. 5b})$$

EXPERIMENTAL

In the current study, II was investigated in humans. The volumes in the compartments and the blood flows were estimated from the anatomical-physiological values for a 70-kg human. Since these values were not the weights of the selected subjects, these parameters were adjusted linearly for variations in the size of the patient. The volumes and blood flows were taken from Dedrick *et al.* (7), who found it necessary to adjust the volume of the lean compartment to explain adequately the pharmacokinetics of I. The lean compartment volume was so adjusted in the present model. The Michaelis constant, deaminase activity, and kidney clearance constant for I were also taken from Dedrick *et al.* (8).

Ho (16) presented *in vitro* hydrolysis data for II to I in human plasma, showing that the hydrolysis was first order in II concentration. Thus, it was assumed here that the hydrolysis *in vivo* is first order and that the *in vivo* hydrolysis rate can be estimated from the *in vitro* data, yielding a hydrolysis rate constant of 0.005 min^{-1} . When this constant was fitted into this model, it was too low to explain the appearance of I. Thus, the hydrolysis rate constant was adjusted to mirror accurately hydrolysis of II to I *in vivo*. Finally, the clearance of II was estimated from cumulative excretion data developed by Ho *et al.* (17, 18).

All parameters used in the models (Table I) were estimated from *in vivo* data, with the exception of the urinary clearances, which were estimated from *in vivo* cumulative excretion curves, and the hydrolysis rate constant, which was estimated from *in vitro* data and adjusted to reflect *in vivo* hydrolysis.

RESULTS AND DISCUSSION

The data modeled here are the data of Ho *et al.* (17, 18), where plasma concentration curves for II and I were represented as a function of time after mixed intravenous injections for several subjects. Only one subject is presented here. Several other subjects were modeled by altering the

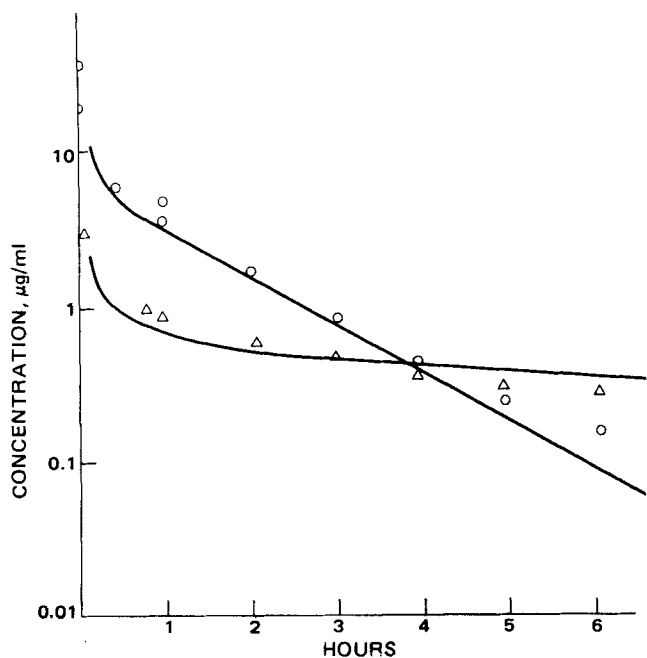


Figure 1—Plasma concentration in 70-kg human after $2.84 \times 10^5 \mu\text{g}$ iv of II and $9 \times 10^4 \mu\text{g}$ iv of I. Hydrolysis rate = 0.01 min^{-1} . Key: Δ , I; and \circ , II.

organ volumes and flow rates to reflect differences in subject sizes. Similar results to those discussed were obtained.

Figure 1 represents the plasma disappearance curve of II and I from blood in a human subject after an intravenous injection of II. Approximately 24% I is contained in the injection. The I impurity was considered a simultaneous injection with II and thus was included in the model. The solid lines represent the concentration of II and I as predicted by the model using a hydrolysis rate of 0.01 min^{-1} . There is reasonable agreement between the model and the experimental data. The model for I underpredicts the plasma concentration at times after 2 hr.

Figure 2 represents the same data, using the hydrolysis rate constant of 0.005 min^{-1} , the value calculated from *in vitro* data. The agreement in this case is not quite as good, indicating that hydrolysis *in vivo* occurs at a somewhat higher rate than *in vitro*. Figure 3 contains a hypothetical study whereby the concentration of I predicted by the model using an injection of II of the same size as that of Ho *et al.* (17, 18) is compared to a hypothetical injection of an equal mass of I only. Shortly after an injection of I only, the concentration was much higher than the I concen-

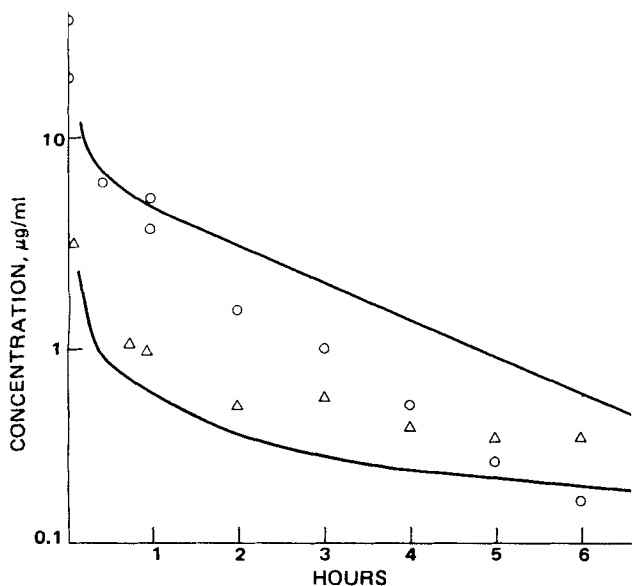


Figure 2—Blood plasma concentration in 70-kg human after $2.84 \times 10^5 \mu\text{g}$ iv of II and $9 \times 10^4 \mu\text{g}$ iv of I. Hydrolysis rate = 0.005 min^{-1} . Key: Δ , I; and \circ , II.

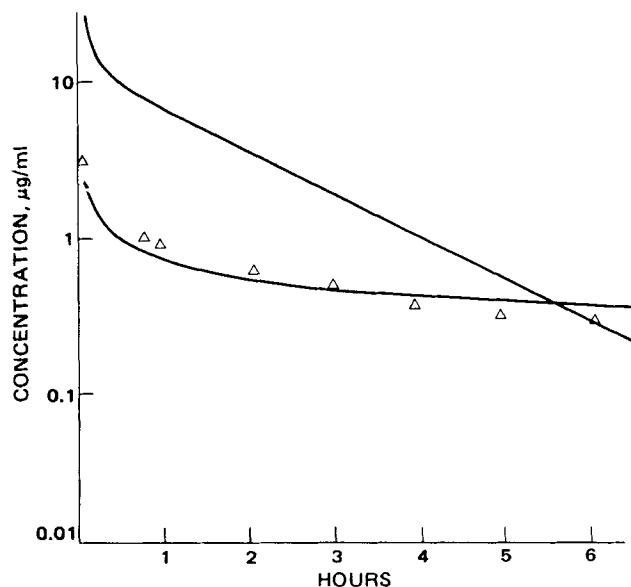


Figure 3—Plasma I concentration in 70-kg human after simulated intravenous injection of equal masses of I and II. Key: upper curve, I alone; and lower curve, I from II.

tration due to both hydrolysis and impurity from an injection of II. However, at later times, the II injection provided for a higher concentration of I. This effect may be more apparent during times for which data were unavailable.

As previously stated by Ho (16), it is possible, based on pharmacokinetics, that the enhanced therapeutic effect of II is attributable to its action as a pool for I production, since the concentration of I is maintained at a somewhat higher level at longer periods when II is employed rather than I alone. The fact that a simple pharmacokinetic model agrees directly with the experimental results by the inclusion of a first-order hydrolysis term ascertained qualitatively *in vitro* supports this hypothesis. Since the main goal of therapy with either II or I is to maintain a concentration of I above the therapeutic level for as long as possible without toxic effects caused by high I concentrations, the model presented allows the manipulation and study of various dosage regimens prior to clinical application.

REFERENCES

- (1) A. P. Bodey, E. J. Preireich, R. W. Monto, and J. S. Hewett, *Cancer Chemother. Rep.*, **53**, 59 (1969).
- (2) R. R. Ellison, T. A. Silver, T. F. Holland, M. Weil, C. Jacquiliat, M. Boirow, J. Bernard, A. Sawitsky, F. Rosner, B. Gussoff, R. T. Silver, A. Karanas, F. Haurani, R. Kyle, J. L. Hutchison, R. J. Forcier, J. H. Moon, J. Cuttler, C. L. Spurr, D. M. Hayes, J. Blom, and L. A. Leone, *Blood*, **32**, 507 (1968).
- (3) R. W. Talley and V. K. Vaitkevicius, *ibid.*, **21**, 352 (1963).
- (4) A. Hoshi, R. Kanzaw, K. Kuretani, M. Saneyoshi, and Y. Arai, *Gann*, **62**, 145 (1971).
- (5) J. M. Vanditti, M. C. Baratta, N. Greenberg, B. J. Abbott, and I. Kline, *Cancer Chemother. Rep.*, **56**, 483 (1972).
- (6) J. P. Howard, N. Geuik, and M. L. Murphy, *ibid.*, **50**, 287 (1966).
- (7) R. L. Dedrick, D. D. Forrester, J. N. Cannon, S. W. El Darrer, and L. B. Mellett, *Biochem. Pharmacol.*, **22**, 2405 (1973).
- (8) R. L. Dedrick, D. D. Forrester, and D. H. W. Ho, *ibid.*, **21**, 1 (1972).
- (9) K. B. Bischoff and R. L. Dedrick, *J. Pharm. Sci.*, **57**, 1346 (1968).
- (10) K. B. Bischoff, R. L. Dedrick, and D. S. Zaharko, *ibid.*, **59**, 149 (1970).
- (11) K. B. Bischoff and R. L. Dedrick, *J. Theoret. Biol.*, **29**, 63 (1970).
- (12) K. B. Bischoff, R. L. Dedrick, D. S. Zaharko, and J. A. Longstreth, *J. Pharm. Sci.*, **60**, 1128 (1971).
- (13) R. L. Dedrick and K. B. Bischoff, *Chem. Eng. Prog. Symp. Ser.*, **84**, 32 (1968).
- (14) R. L. Gabelnick, R. L. Dedrick, and R. S. Bourke, *J. Appl. Physiol.*, **28**, 636 (1970).

- (15) P. Harris and J. F. Gross, *Cancer Chemother. Rep., Part 1, No. 4*, 59, 819 (1975).
 (16) D. H. Ho, *Biochem. Pharmacol.*, 23, 1235 (1974).
 (17) D. H. W. Ho, V. Rodriguez, T. L. Loo, G. P. Bodgy, and E. J. Freireich, *Clin. Pharmacol. Ther.*, 17, 66 (1975).
 (18) D. H. W. Ho, C. J. K. Carter, T. L. Loo, R. L. Abbott, and C. M. McBride, *Drug Metab. Dispos.*, 3, 309 (1976).
 (19) G. W. Camiener, *Biochem. Pharmacol.*, 16, 1981 (1967).
 (20) G. W. Camiener and C. G. Smith, *ibid.*, 14, 1405 (1965).

ACKNOWLEDGMENTS AND ADDRESSES

Received October 29, 1976, from the **Department of Chemical and Petroleum Engineering, University of Kansas, Lawrence, KS 66045*, and the †*Department of Chemical Engineering, University of Arizona, Tucson, AZ 85721*.

Accepted for publication January 6, 1977.

Supported in part by HEW Grant HL 17421.

* To whom inquiries should be directed.

Mass Spectrometry of Cannabinoids

T. B. VREE

Abstract □ The mechanism of fragmentation of cannabinoids to fragments m/e 314, 299, 271, 258, 246, 243, and 231 is given. Cannabidiol, cannabindiol, cannabinol, Δ^6 - and Δ^1 -tetrahydrocannabinol, cannabichromene, cannabicyclol, derivatives with pentyl, propyl, and methyl side chains, their methyl ethers, and *cis-trans* and *ortho-para* isomers were analyzed by GLC-mass spectrometry using different energies for fragmentation during GLC elution. The following mechanism was distinguished: loss of a methyl radical, ring closure and rotation, McLafferty rearrangement, retro Diels-Alder, internal protonation, isomerization and internal bond formation, and one-step fragmentation to m/e 231.

Keyphrases □ Cannabinoids, various—mechanism of mass spectrometric fragmentation □ Mass spectrometry—mechanism of fragmentation of various cannabinoids

One rapid method of identification of cannabinoids is combined GLC-mass spectrometry. The mass spectra of cannabinoids can be distinguished from each other. The fragmentation process is relatively slow for most compounds, taking 40–50 ev before completion, after which the relative intensities of the fragments do not alter (Fig. 1). When the relative intensities of each particular mass fragment are plotted against the electron energy used, the fragmentation process can be characterized for each cannabinoid.

In the 10–20-ev range, the fragmentation just starts; differences in this process between the different structures

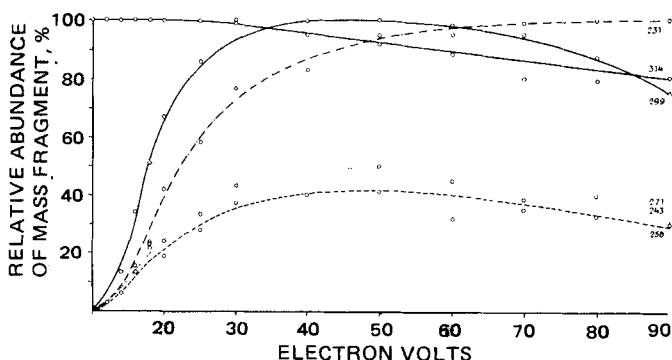


Figure 1—Electron voltage mass fragmentogram of trans-para-Vb. Fragments are formed relatively slowly between 10 and 30 ev. In this particular interval, small structural differences of the cannabinoids may result in big differences in the formation rate of certain mass fragments.

are then relatively large. The technique of taking mass spectra at different electron voltages between 10 and 20 ev and plotting relative intensities against electron volts gives very characteristic electron voltage mass fragmentograms of the cannabinoids, which, for instance, led to the discovery of some propyl and methyl homologs of the known cannabinoids. This method is also useful in elucidating the various cannabinoid fragmentation pathways.

EXPERIMENTAL

Materials and Methods—A gas chromatograph-mass spectrometer¹ was used. Glass columns, 1.80 m × 4 mm i.d., were packed with 3% OV-17 on 60–80-mesh Gas Chrom Q. The temperatures were: oven, 200°; separator, 220°; and ion source, 250°. The helium flow was 20 ml/min. Repetitive mass spectra were taken at 20, 18, 16, 14, 12, and 10 ev during the elution of a GLC peak. The detector gain was increased in the 16–10-ev energy interval. The trap current was 60 μ amp, and the accelerating voltage was 3.5 kv. The pressure in the analyzer tube was 2×10^{-6} Torr.

The gas chromatograms were recorded by a total-ion current monitor at 20 ev. Gas chromatograms of mixtures of natural and synthetic cannabinoids were published elsewhere (1). The mass spectra obtained were normalized, and the relative abundance of a particular mass fragment was plotted against the electron voltage.

Cannabinoids²—Lebanese, Nepalese, Moroccan, Columbian, Indonesian, and Congolese hashish samples and marijuana samples from Brazil and South Africa were powdered and extracted with ether or *n*-hexane by homogenizing for 10 min. After filtration of the extracts, most of the solvent was evaporated to give suitable concentrations for GLC-mass spectrometry. Synthetic samples were only dissolved in a small aliquot of ether.

RESULTS

Molecular Ion m/e 314—The aryl nucleus is the center of charge localization, and elimination of an electron from this nucleus gives the molecular ion m/e 314. At 10 ev, the molecular ion m/e 314 is the base peak. At 20 ev, large differences in the relative intensities between different cannabinoids can be observed (Table I).

Formation of Mass Fragment M - 15 (m/e 299 and 295)—The loss of the geminal methyl group, which nearly all structures have in common,

¹ LKB 9000.

² Natural Cannabis samples were obtained from and identified by Dr. A. H. Witte, Laboratory of Forensic Sciences, Ministry of Justice, The Hague, The Netherlands, and Dr. E. A. Carlini, Depto de Psicobiologia, Escola Paulista de Medicina, Sao Paulo, Brazil. Synthetic cannabinoids were a gift from Dr. T. Petrzilka, Eidgen. Hochschule Zurich, Department of Organic Chemistry, Zurich, Switzerland, where voucher specimens were deposited.